A Thermodynamic Interpretation of the "Excluded-Volume Effect" in Coupled Diffusion

Pellumb Jakupi, Helga Halvorsen, and Derek G. Leaist*

Department of Chemistry, University of Western Ontario, London, Ontario N6A 5B7, Canada

Received: July 31, 2003; In Final Form: November 24, 2003

Strongly coupled diffusion has been reported for fluxes of solutes that differ significantly in molecular size. According to the excluded-volume model, a solute increases the effective concentrations of other solutes by reducing the volume of solution they can occupy. The flux of solute 2 produced by the gradient ∇c_1 in the concentration of solute 1 is interpreted as the ordinary diffusion of solute 2 down its effective concentration gradient. Cross-diffusion coefficient $D_{21} = D_{22}c_2V_{1,\text{eff}}/(1 - c_1V_{1,\text{eff}})^2$ is predicted, where $V_{1,\text{eff}}$ is the effective molar volume of solute 1. This model does not account for countercurrent coupled diffusion ($D_{21} < 0$) and is found to be inconsistent with the Onsager reciprocal relation (ORR). A thermodynamic model of coupled transport is developed by approximating the flux of solute *i* as the product of its concentration, mobility, and chemical potential gradient driving force ($-\nabla\mu_i$), which gives $D_{21} = D_{22}c_2(V_1 - V_0)/[1 - c_1(V_1 - V_0)]$, where V_i is the partial molar volume of component *i* and the solvent is component 0. For dilute solutions with $V_1 \gg V_0$, the thermodynamic prediction $D_{21} \approx c_2V_1D_{22}$ and the excluded-volume prediction $D_{21} \approx c_2V_{1,\text{eff}}D_{22}$ are qualitatively similar, but the thermodynamic model does not require the assumption of effective concentrations or effective volumes, provides a physical explanation for coupled diffusion, and is consistent with the ORR. Moreover, because $\partial\mu_2/\partial c_1$ is proportional to $V_1 - V_0$, the thermodynamic model suggests that a concentration gradient in solute 1 can drive co-current or counter-current flows of solute 2, depending on the relative volumes of solute 1 and solvent 0. These features are illustrated by comparing measured and predicted D_{ik} coefficients for solutions of *n*-octane(1) + *n*-hexadecane(2) in *n*-dodecane(0) at nine different compositions at 25 °C.

Introduction

Recent work has drawn attention to the strongly coupled diffusion of solutes that differ significantly in molecular size.[1−10] Gradients in the concentration of macromolecular solutes are particularly effective at driving coupled fluxes of other solutes. A striking example of this behavior is provided by aqueous solutions of lysozyme (∼10 500 $cm^3\ mol^{-1}$) + poly(ethylene glycol) (PEG400, ∼400 $g\ mol^{-1}$ and 340 $cm^3\ mol^{-1}$).[1] Reported ternary mutual diffusion coefficients for this system indicate that a lysozyme concentration gradient can drive a co-current coupled flux of 35 mol of PEG400 per mole of lysozyme driven by its own concentration gradient. Vergara et al.[1] have discussed possible causes of this remarkable behavior. They conclude that the large fluxes of PEG400 driven by lysozyme concentration gradients is an excluded-volume effect. The excluded-volume effect has also been used to interpret coupled mutual diffusion in ternary aqueous solutions of lysozyme + NaCl,[2−4] PEG400 + NaCl,[5] poly(vinylpyrrolidone) + alkylsulfonate surfactant,[6] tetraethylene glycol (EG4) + diethylene glycol (EG2),[7] EG5 + EG3,[8] EG6 + EG2,[9] and PEG2000 + PEG200.[10]

The excluded-volume model of multicomponent mutual diffusion is based on the assumption that a solute increases the "effective" concentrations of other solutes by reducing the volume of solution they can occupy.[1−4] In a ternary solution of solute 1 + solute 2 + solvent 0, for example, the coupled flux of solute 2 driven by the gradient ∇c_1 in the concentration of solute 1 is identified as the "ordinary" diffusion of solute 2 down the gradient in its effective concentration produced by the gradient in solute 1. This interpretation of coupled diffusion, though intuitively appealing, raises several questions. If added solute 1 increases the effective concentration of solute 2 by reducing the volume of solution that can be occupied by solute 2, then the volume of solution that can be occupied by the solvent component is also reduced, and an increase in the effective solvent concentration might reasonably be expected. The effective solvent concentration in this case $c_{0,\text{eff}} = c_0/(1 - c_1V_{1,\text{eff}})$ is the stoichiometric solvent concentration c_0 divided by the effective volume fraction of solution $1 - c_1V_{1,\text{eff}}$ not occupied by solute 1, where $V_{1,\text{eff}}$ denotes the effective molar volume solute 1. Combining the definition of $c_{0,\text{eff}}$ with the identity $V_0\nabla c_0 = -V_1\nabla c_1$ (at constant c_2) leads to the result $\nabla c_{0,\text{eff}} = 0$ for dilute solutions ($c_0V_0 \approx 1$), implying zero flux of solvent in the volume-fixed frame of reference. In effect, the diffusion of solvent down its stoichiometric concentration gradient is canceled by the assumed co-current coupled flow of solvent driven down its effective concentration gradient produced by added solute 1. Mutual diffusion, however, requires equal volume fluxes of solvent and solute moving in opposite directions to maintain zero bulk flow.[11,12] The role played by the solvent concentration gradient in coupled diffusion, which is not included in the excluded-volume model, is discussed later in this paper.

More significantly, the fundamental driving forces for mutual diffusion are chemical potential gradients,[11,12] not concentration gradients (real or imagined). If an increase in the concentration of a solute is assumed to drive co-current coupled flows of the other solution components by increasing their effective con-

* Corresponding author. Telephone: (519) 661-2166 ext 86317. Fax: (519) 661-3022. E-mail: dleaist@uwo.ca.

10.1021/jp030951+ CCC: $27.50
Published on Web 05/08/2004

centrations, then increases in the chemical potentials of these components are reasonably expected, together with an increase in the chemical potential of the added solute. According to the Gibbs−Duhem relation,[12,13] however, the chemical potentials of solution components cannot simultaneously increase at constant temperature and pressure the conditions of mutual diffusion measurements.

In connection with this point, thermodynamic studies of multicomponent solutions[12−15] demonstrate that the chemical potential of a given solute can increase, decrease, or remain unchanged if the concentration of another solute is raised, even for ideal solutions. Thermodynamics therefore provides driving forces for both co-current and counter-current coupled diffusion flows. In contrast, only co-current coupled diffusion is predicted by excluded-volume theory, which does not account for counter-current coupled diffusion reported for polystyrene + toluene + cyclohexane solutions,[16] ideal ternary solutions,[17] and for several other systems where the excluded-volume model should apply.[18−20] Moreover, the excluded-volume effect does not appear to have been related to the accepted driving forces for mutual diffusion.

Prompted by these considerations, the present work is an attempt to provide a physical explanation for the coupled diffusion of solutes caused by differences in molecular size. The approach used here is to approximate the flux of a solute as the product of its concentration, mobility, and chemical potential gradient driving force. Coupled diffusion predicted by this thermodynamic model is compared with excluded-volume predictions. Both models are checked for consistency with the Onsager reciprocity relation (ORR).[11,21]

Ternary mutual diffusion coefficients for solutions of *n*-octane(1) + *n*-hexadecane(2) in *n*-dodecane(0) are reported in this paper to provide an experimental test of the coupled-diffusion models. Alkane mixtures are in many respects systems of choice for testing simple theories of liquid diffusion.[19,22,23] Transport in these systems is not complicated by hydration, polydispersity, or molecular association. Equally important, *n*-alkane mixtures are nearly ideal in the thermodynamic sense, so coupled diffusion driven by specific solvent−solute and solute−solute interactions (e.g., salting-in" or "salting-out" effects[24,25]) and the related activity-coefficient terms are small or negligible, even for concentrated solutions with relatively large volume fractions of solute. Diffusion data for *n*-alkane solutions can therefore provide a cleaner and more convincing test of the relation between coupled diffusion and molecular size than reported hitherto. Conveniently for the present study, the molar volumes of *n*-alkane components can be adjusted by changing the alkane chain length.

Experimental Section

In the notation used here, ternary mutual diffusion coefficient D_{ik} gives the molar flux J_i of solute i in the volume-fixed reference frame produced by the gradient in the concentration of solute k.

$$J_1 = -D_{11}\nabla c_1 - D_{12}\nabla c_2 \tag{1}$$

$$J_2 = -D_{21}\nabla c_1 - D_{22}\nabla c_2 \tag{2}$$

D_{ik} coefficients for solutions of *n*-octane(1) + *n*-hexadecane-(2) in *n*-dodecane were measured at 25.00 (±0.05) °C by the Taylor dispersion method.[11,26,27] Solutions were prepared by mixing weighed amounts of *n*-alkanes (Aldrich anhydrous products, purity >99%). Volumetric concentrations were calculated using densities measured with an Anton Paar DMA 50 vibrating-tube density meter (accuracy ± 0.00001 g cm^{-3}).

At the start of each dispersion run, a Teflon injection valve (Rheodyne model 50) was used to introduce 0.020 cm^3 of solution of composition $\bar{c}_1 + \Delta c_1$, $\bar{c}_2 + \Delta c_2$ into a laminar carrier stream of composition $\bar{c}_1$, $\bar{c}_2$. A liquid-chromatography differential refractometer detector (Shimadzu model RID-10A, sensitivity 10^{-8} refractive index units) monitored the dispersion profiles at the outlet of a Teflon capillary tube (length 1600 cm, internal radius $r = 0.0406_0$ cm). Retention times t_R were typically 7×10^3 s to 8×10^3 s. The refractometer output voltage $V(t)$ was measured at 3-second intervals by a computer-controlled digital voltmeter (Hewlett-Packard model 3478A).

The dispersion profiles were analyzed by fitting the equation[27]

$$V(t) = B_0 + B_1 t + V_{\max}\sqrt{\frac{t_R}{t}}\sum_{i=1}^{2} P_i \exp\left[-\frac{12D^{(i)}(t-t_R)^2}{r^2 t}\right] \tag{3}$$

to the measured detector voltages. B_0 and B_1 are the baseline voltage and baseline slope, $V_{\max}$ is the peak height, and $D^{(i)}$ are the eigenvalues of the matrix of D_{ik} coefficients. The normalized pre-exponential factors ($P_1 + P_2 = 1$)

$$P_i = \frac{w_i\sqrt{D^{(i)}}}{w_1\sqrt{D^{(1)}} + w_2\sqrt{D^{(2)}}} \tag{4}$$

are related to the initial concentration differences by

$$w_1 = a + b\alpha_1 \tag{5}$$

$$w_2 = 1 - w_1 \tag{6}$$

where α_1 denotes the fraction of the refractive-index difference generated by the initial concentration difference in component 1

$$\alpha_1 = \frac{R_1\Delta c_1}{R_1\Delta c_1 + R_2\Delta c_2} \tag{7}$$

where a and b are constants for each carrier solution and $R_i = \partial n/\partial c_i$ gives the change in the refractive index n per unit change in the concentration of alkane component i. α_1 was calculated using values of R_2/R_1 obtained from the corresponding ratio of peak areas divided by the excess concentration of component 1 or 2 in the injected solution samples. Equation 3 was fitted to pairs of dispersion peaks generated by injecting excess component 1 ($\alpha_1 = 1$) or excess component 2 ($\alpha_1 = 0$) into each carrier solution. B_0, B_1, $V_{\max}$, and t_R were used as adjustable least-squares parameters for each profile, together with $D^{(1)}$, $D^{(2)}$, a, and b for each pair of profiles.

Ternary dispersion profiles resemble two overlapping Gaussian peaks with variances $r^2t_R/24D^{(1)}$ and $r^2t_R/24D^{(2)}$. For initial conditions satisfying $a + b\alpha_1^{(1)} = P_1 = 1$, however, the Gaussian in $D^{(2)}$ vanishes. The concentration differences $\alpha_1^{(1)}/R_1$, $(1 - \alpha_1^{(1)})/R_2$ are therefore an eigenvector of the matrix of D_{ik} coefficients, with eigenvalue $D^{(1)}$. Similarly, the Gaussian in $D^{(1)}$ vanishes for initial conditions, satisfying $a + b\alpha_1^{(2)} = P_1 = 0$, and $\alpha_1^{(2)}/R_1$, $(1 - \alpha_1^{(2)})/R_2$ is an eigenvector of $\boldsymbol{D}$ with eigenvalue $D^{(2)}$. Using the measured eigenvalues and eigenvectors, the matrix of ternary D_{ik} coefficients is readily constructed by a similarity transform.[27]

$$D_{11} = D^{(1)} + \frac{a(1-a-b)}{b}(D^{(1)} - D^{(2)}) \quad (8)$$

$$D_{12} = \frac{R_2}{R_1}\frac{a(1-a)}{b}(D^{(1)} - D^{(2)}) \quad (9)$$

$$D_{21} = \frac{R_1}{R_2}\frac{(a+b)(1-a-b)}{b}(D^{(2)} - D^{(1)}) \quad (10)$$

$$D_{22} = D^{(2)} + \frac{a(1-a-b)}{b}(D^{(2)} - D^{(1)}) \quad (11)$$

The concentrations of each *n*-alkane component in the injected solution samples and the carrier solutions differed by ≤ 0.15 mol dm^{-3}. Within this range of initial concentration differences, the measured D_{ik} coefficients were independent of Δc_i and therefore represented differential values at the composition of the carrier solution.

Theory

In this section the excluded-volume interpretation of coupled diffusion is briefly summarized followed by the development of the thermodynamic model. Ideal solutions of nonelectrolytes at constant temperature and pressure are assumed throughout.

Excluded-Volume Model of Coupled Diffusion. According to this model, the effective concentration of solute 2 in a ternary solution is its actual concentration c_2 divided by the effective volume fraction of solution not occupied by solute 1.

$$c_{2,\text{eff}} = \frac{c_2}{1 - c_1 V_{1,\text{eff}}} \quad (12)$$

The coupled flux of solute 2 caused by the gradient in the concentration of solute 1

$$J_2(\nabla c_2 = 0) = -D_{21}\nabla c_1 = -D_{22}\nabla c_{2,\text{eff}} \quad (13)$$

is attributed to the main diffusion of solute 2 down the gradient $\nabla c_{2,\text{eff}}$ in its effective concentration produced by the concentration gradient in solute 1.

$$\nabla c_{2,\text{eff}} = \left(\frac{\partial c_{2,\text{eff}}}{\partial c_1}\right)_{c_2} \nabla c_1 = -\frac{c_2 V_{1,\text{eff}}}{(1 - c_1 V_{1,\text{eff}})^2}\nabla c_1 \quad (14)$$

Substituting eq 14 for $\nabla c_{2,\text{eff}}$ into eq 13 provides the excluded-volume expression[1−10]

$$D_{21} = \frac{c_2 V_{1,\text{eff}}}{(1 - c_1 V_{1,\text{eff}})^2} D_{22} \quad (15)$$

for cross-coefficient D_{21}. In agreement with experiment, large positive D_{21} values are predicted in cases where solute 1 is macromolecular and $V_{1,\text{eff}}$ is therefore relatively large. For solutions dilute in solute 1, the volume fraction of solute 1 is small ($c_1 V_{1,\text{eff}} \ll 1$) and eq 15 simplifies to $D_{21} \approx c_2 V_{1,\text{eff}} D_{22}$.

Similar considerations lead to the excluded-volume expression[1,5,6,8−10]

$$D_{12} = \frac{c_1 V_{2,\text{eff}}}{(1 - c_2 V_{2,\text{eff}})^2} D_{11} \quad (16)$$

for cross-coefficient D_{12}, and hence $D_{12} \approx c_1 V_{2,\text{eff}} D_{11}$ for dilute solutions of solute 2 ($c_2 V_{2,\text{eff}} \ll 1$).

Thermodynamic Model of Coupled Diffusion. The diffusion velocity v_i of solute *i* can be approximated as the product of its mobility u_i and chemical potential gradient driving force, $-\nabla\mu_i$, which gives[11,121]

$$J_i = c_i v_i = -c_i u_i \nabla\mu_i \quad (17)$$

for the flux of solute *i*. This well-known result can be used to estimate the coupled flux of solute 2 produced by a concentration gradient in solute 1 by substituting $\nabla\mu_2 = (\partial\mu_2/\partial c_1)_{c2}\nabla c_1$ into eq 17.

$$J_2(\nabla c_2 = 0) = -D_{21}\nabla c_1 = -c_2 u_2 \left(\frac{\partial\mu_2}{\partial c_1}\right)_{c_2} \nabla c_1 \quad (18)$$

The corresponding expression for the flux of solute 2 produced by its own concentration gradient

$$J_2(\nabla c_1 = 0) = -D_{22}\nabla c_2 = -c_2 u_2 \left(\frac{\partial\mu_2}{\partial c_2}\right)_{c_1} \nabla c_2 \quad (19)$$

is obtained by substituting $\nabla\mu_2 = (\partial\mu_2/\partial c_2)_{c_1}\nabla c_2$ into eq 17. Dividing eq 18 by eq 19 gives the thermodynamic expression

$$D_{21} = \frac{(\partial\mu_2/\partial c_1)_{c_2}}{(\partial\mu_2/\partial c_2)_{c_1}} D_{22} \quad (20)$$

for cross-coefficient D_{21}. This expression for D_{21} is not new. Similar results have been derived in a previous study of coupled diffusion in ideal ternary solutions.[17] Eq 20 has also been used to estimate coupled diffusion fluxes produced by nonideal solution thermodynamics ("salting-out").[28] In the present study, eq 20 is used to investigate coupled diffusion caused by differences in the sizes of solute and solvent molecules.

A gradient in the concentration of solute 1 can provide a thermodynamic driving force for a coupled flow of solute 2 if a change in the concentration of solute 1 produces a change in the chemical potential of solute 2. Thus cross-derivatives such as $(\partial\mu_2/\partial c_1)_{c_2}$ play a key role in the thermodynamic model of coupled diffusion. The thermodynamic activity a_i and mole fraction X_i of component *i* are identical for ideal nonelectrolyte solutions.[13] For an ideal solution of solvent 0 + solute 1 + solute 2, the activity and chemical potential of solute 2 are related to the concentrations of the solution components as follows

$$a_2 = X_2 = c_2/(c_0 + c_1 + c_2) \quad (21)$$

$$\mu_2 = \mu_2^* + RT \ln [c_2/(c_0 + c_1 + c_2)] \quad (22)$$

where R is the gas constant and μ_2^* (the chemical potential of pure liquid component 2) is a constant at a given pressure and temperature T.

Differentiation of eq 22

$$\frac{1}{RT}\left(\frac{\partial\mu_2}{\partial c_1}\right)_{c_2} = -\frac{1 + (\partial c_0/\partial c_1)_{c_2}}{c_0 + c_1 + c_2} \quad (23)$$

and using $(\partial c_0/\partial c_1)_{c_2} = -V_1/V_0$ from the relation $V_0\, dc_0 + V_1\, dc_1 + V_2\, dc_2 = 0$ (obtained[29] by combining the definition $V_0 c_0 + V_1 c_1 + V_2 c_2 = 1$ with the Gibbs−Duhem relation $c_0\, dV_0 + c_1\, dV_1 + c_2\, dV_2 = 0$) gives

$$\frac{1}{RT}\left(\frac{\partial\mu_2}{\partial c_1}\right)_{c_2} = \frac{(V_1/V_0) - 1}{c_0 + c_1 + c_2} \tag{24}$$

This is a key result for the thermodynamic model of coupled diffusion. It shows that a gradient in the concentration of solute 1 can produce a thermodynamic driving force for solute 2, *even for ideal solutions in which the concentration of solute 2 is constant*. Of additional interest, eq 24 shows that increasing the concentration of solute 1 can raise the chemical potential of solute 2 (if $V_1 > V_0$) or lower the chemical potential of solute 2 (if $V_1 < V_0$) depending on the relative partial molar volumes of the solvent 0 and solute 1. Ideal-solution thermodynamics can therefore provide driving forces for co-current and counter-current coupled flows of solutes.

Equation 24 has interesting implications for coupled diffusion caused by concentration gradients in macromolecular solutes. In cases where $V_1 \gg V_0$, each molecule of added solute 1 displaces many solvent(0) molecules. An increase in the concentration of macromolecular solute 1 therefore produces a much larger decrease in the solvent concentration [$dc_0 = -(V_1/V_0)\, dc_1$ at constant c_2], which in turn significantly reduces the total molar concentration $c_0 + c_1 + c_2$ and substantially increases in the activity $c_2/(c_0 + c_1 + c_2)$ of solute 2. Indeed, $(RT)^{-1}(\partial\mu_2/\partial c_1)_{c_1} \approx V_1$ for dilute solutions ($c_0V_0 \approx 1$) with $V_1 \gg V_0$. By this thermodynamic mechanism, a gradient in the concentration of a macromolecular solute can provide a strong driving force for co-current coupled flows of other solutes. Gradients in solvent concentration and gradients in solvent chemical potential are not included in the excluded-volume model of coupled diffusion.

Differentiation of eq 22 for μ_2

$$\frac{1}{RT}\left(\frac{\partial\mu_2}{\partial c_2}\right)_{c_1} = \frac{1}{c_2} + \frac{(V_2/V_0) - 1}{c_0 + c_1 + c_2} \tag{25}$$

and substituting this result and eq 24 into eq 20 gives the expression

$$D_{21} = \frac{c_2(V_1 - V_0)}{1 - c_1(V_1 - V_0)} D_{22} \tag{26}$$

for cross-coefficient D_{21} predicted by the thermodynamic model. Similar considerations lead to the thermodynamic expressions

$$D_{12} = \frac{(\partial\mu_1/\partial c_2)_{c_1}}{(\partial\mu_1/\partial c_1)_{c_2}} D_{11} \tag{27}$$

$$D_{12} = \frac{c_1(V_2 - V_0)}{1 - c_2(V_2 - V_0)} D_{11} \tag{28}$$

for cross-coefficient D_{12}.

For dilute solutions ($c_1 \approx 0$ and $c_2 \approx 0$), the thermodynamic expressions for the cross-coefficients simplify to $D_{12} = c_1(V_2 - V_0)D_{11}$ and $D_{21} = c_2(V_1 - V_0)D_{22}$. If in addition solute 1 is macromolecular ($V_1 \gg V_0$), the predicted D_{21} value simplifies further to $c_2V_1D_{22}$, in qualitative agreement with the excluded-volume prediction $c_2V_{1,\mathrm{eff}}D_{22}$.

The partial molar volumes V_i in the expressions for cross-coefficients D_{12} and D_{21} predicted by the thermodynamic model of coupled diffusion (eqs 26 and 28) arise from the thermodynamic derivatives $\partial\mu_i/\partial c_k$ (eqs 24 and 25). Effective hydrodynamic volumes of the diffusing solutes are not used explicitly in the thermodynamic model of coupled diffusion (in contrast to the $V_{i,\mathrm{eff}}$ values used in the excluded-volume model). However, effective hydrodynamic volumes are included implicitly in the thermodynamic model by using measured D_{11} and D_{22} values to evaluate the mobility of each solute (see eqs 18 and 19).

Onsager Reciprocal Relation (ORR). Coupled Fick equations such as eqs 1 and 2 are frequently used in studies of multicomponent mutual diffusion. Fick descriptions of diffusion, though convenient in practice, are not unique. Onsager's equations[11,21,24] provide a more fundamental description of mutual diffusion by relating diffusion fluxes to the thermodynamic driving forces.

$$J_i = -\sum_{k=1}^{N} L_{ik}\nabla\mu_{ik} \tag{29}$$

In addition, the Onsager $L_{ik(0)}$ coefficients defined for solvent-fixed diffusion fluxes $J_{i(0)}$

$$J_{i(0)} = -\sum_{k=1}^{N} L_{ik(0)}\nabla\mu_{ik} \tag{30}$$

obey the Onsager reciprocal relation (ORR) $L_{ik(0)} = L_{ki(0)}$ ($i \neq k$).

The ORR for ternary solutions ($N = 2$) places the restriction[11,12]

$$D_{12(0)}\left(\frac{\partial\mu_1}{\partial c_1}\right)_{c_2} - D_{11(0)}\left(\frac{\partial\mu_1}{\partial c_2}\right)_{c_1} = D_{21(0)}\left(\frac{\partial\mu_2}{\partial c_2}\right)_{c_1} - D_{22(0)}\left(\frac{\partial\mu_2}{\partial c_1}\right)_{c_2} \tag{31}$$

on the solvent-fixed ternary mutual diffusion coefficients ($D_{ik(0)}$ in the notation used here). The solvent-fixed and volume-fixed ternary mutual diffusion coefficients are related as follows[30]

$$D_{ik(0)} = D_{ik} + \frac{c_i}{c_0V_0}\sum_{q=1}^{2} V_qD_{qk}\ (i = 1, 2;\ k = 1, 2) \tag{32}$$

Measured D_{ik} coefficients can be checked for consistency with the ORR[11,30] using accurate experimental values of V_i and $\partial\mu_i/\partial c_k$ together with eqs 31 and 32. For the nonelectrolyte systems relevant to the present study, dilute solutions ($c_1V_1 \ll 1$ and $c_2V_2 \ll 1$) can be reliably considered ideal. Under these conditions $\partial\mu_2/\partial c_1$ and $\partial\mu_2/\partial c_2$ can be accurately evaluated using eqs 24 and 25. The corresponding expressions for the evaluation of $\partial\mu_1/\partial c_2$ and $\partial\mu_1/\partial c_1$ are readily obtained by permuting subscripts 1 and 2 in eqs 24 and 25. At low solute concentrations, moreover, it is well known that the solvent-fixed and volume-fixed frames differ negligibly ($D_{ik(0)} = D_{ik}$, see eq 32) and hence

$$D_{12}\left(\frac{\partial\mu_1}{\partial c_1}\right)_{c_2} - D_{11}\left(\frac{\partial\mu_1}{\partial c_2}\right)_{c_1} = D_{21}\left(\frac{\partial\mu_2}{\partial c_2}\right)_{c_1} - D_{22}\left(\frac{\partial\mu_2}{\partial c_1}\right)_{c_2} \tag{33}$$

for dilute solutions. Substituting the expressions for D_{12} and D_{21} from the thermodynamic model (eqs 26 and 28) into eq 33 together with the expressions for $\partial\mu_i/\partial c_k$ shows that the left and right sides of eq 33 are identically zero. The cross-diffusion coefficients predicted by thermodynamic model of coupled diffusion are therefore consistent with the ORR, at least for ideal dilute solutions where the concentration derivatives of the chemical potentials can be reliably estimated. This result can be understood by noting that the thermodynamic model of

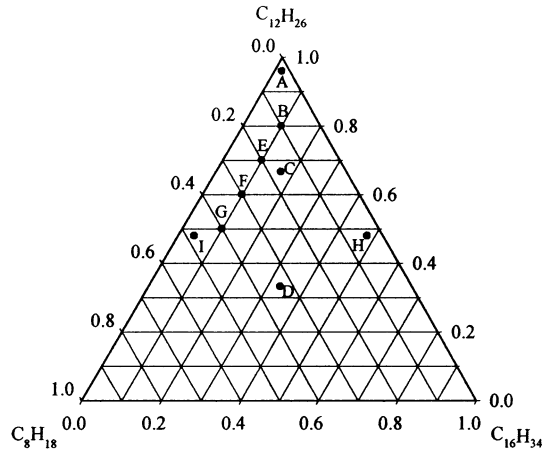

Figure 1. Mole-fraction compositions of the *n*-octane + *n*-hexadecane + *n*-dodecane solutions used for the diffusion measurements.

TABLE 1: Compositions[a] of the Carrier Solutions of *n*-Octane(1) + *n*-Hexadecane(2) in *n*-Dodecane(0) for the Ternary Diffusion Measurements at 25 °C

	X_1	X_2	X_0	$\bar{c}1$	$\bar{c}_2$	$\bar{c}_0$
A	0.0200	0.0200	0.9600	0.0874	0.0875	4.199
B	0.1000	0.1001	0.7999	0.4375	0.4375	3.499
C	0.1666	0.1667	0.6667	0.7288	0.7289	2.916
D	0.3334	0.3333	0.3333	1.4583	1.4578	1.458
E	0.2001	0.1000	0.6999	0.9008	0.4505	3.151
F	0.3000	0.1000	0.6000	1.3918	0.4638	2.784
G	0.4000	0.0999	0.5001	1.9137	0.4783	2.392
H	0.0400	0.4799	0.4801	0.1554	1.8642	1.865
I	0.4799	0.0403	0.4798	2.4004	0.2016	2.400

[a] Units: $\bar{c}_i$ in mol dm^{-3}.

coupled diffusion is based on the approximation that the flux of each solute is proportional to the gradient in its own chemical potential, which is equivalent to the assumption that the Onsager cross-coefficients are zero.

The excluded-volume model of coupled diffusion can also be tested for consistency with the ORR. Substitution of eqs 15 and 16 into eq 33 together with expressions for $\partial\mu_i/\partial c_k$ for ideal dilute solutions gives $(V_{2,\text{eff}} - V_2 + c_0^{-1})D_{11}$ for the left side of eq 33 and $(V_{1,\text{eff}} - V_1 + c_0^{-1})D_{22}$ for the right side of eq 33 in the limit $c_0V_0 \rightarrow 1$. The excluded-volume model of coupled diffusion therefore violates the ORR. This discrepancy arises because effective concentration gradients are inconsistent with chemical potential gradients, the driving forces for mutual diffusion.

Results and Discussion

Solutions of *n*-Octane(1) + *n*-Hexadecane(2) in *n*-Dodecane(0). General considerations recommending *n*-alkane systems for tests of the diffusion models are summarized in the Introduction. Solutions of *n*-octane(1) + *n*-hexadecane(2) with *n*-dodecane(0) as the solvent were chosen in particular to check the prediction that chemical potential gradients can drive counter-current or co-current coupled flows depending on the relative partial molar volumes of solvent and solutes. For this system ($V_1 < V_0$ and $V_2 > V_0$), positive D_{12} values and negative D_{21} values are predicted by the thermodynamic model. In contrast, cross-coefficients can only be positive according to the excluded-volume model.

Ternary D_{ik} coefficients for solutions of *n*-octane(1) + *n*-hexadecane(2) in *n*-dodecane(0) were measured at 25 °C and the mole-fraction compositions plotted in Figure 1. The corresponding volumetric concentrations are listed in Table 1. Equation 3 was fitted to four to eight different sets of dispersion peaks for each carrier solution. The D_{ik} coefficients evaluated from replicate peaks were typically reproducible within ±(0.01 to 0.02) × 10^{-5} cm^2 s^{-1}. The average D_{ik} coefficients for each composition are listed in Table 2.

By definition, D_{12} is zero in the limit $c_1 \rightarrow 0$ (a concentration gradient in *n*-hexadecane(2) cannot produce a coupled flow of *n*-octane(1) in a solution that does not contain *n*-octane(1)). Similarly, D_{21} vanishes in the limit $c_2 \rightarrow 0$. Consistent with this required limiting behavior, the cross-coefficients are zero within experimental precision for the most dilute solution of each solute (composition A). For the more concentrated solutions, cross-coefficients D_{12} and D_{21} increase in magnitude with the concentrations of *n*-octane(1) and *n*-hexadecane(2), respectively. Also, D_{12} is positive and D_{21} is negative, as suggested by the thermodynamic model of coupled diffusion.

The measured and predicted values of D_{12} and D_{21} are listed for comparison in Tables 3 and 4. The cross-diffusion coefficients suggested by the thermodynamic model, assuming ideal solutions (eqs 26 and 28), were calculated using the molar volumes of the pure liquid alkanes (163.6, 294.2, and 228.6 cm^3 mol^{-1} for *n*-octane(1), *n*-hexadecane(2), and *n*-dodecane(0), respectively)[31] for the partial molar volumes of the solution components. The effective molar volumes of *n*-octane(1) and *n*-hexadecane(2) ($V_{1,\text{eff}} = 42.2$ cm^3 mol^{-1} and $V_{2,\text{eff}} = 711$ cm^3 mol^{-1}) used in the excluded-volume predictions were estimated from the limiting diffusion coefficients of *n*-octane and *n*-hexadecane in *n*-dodecane [$D_1^\infty = 1.718 \times 10^{-5}$ cm^2 s^{-1} (ref 22, 23) and $D_2^\infty = 0.670 \times 10^{-5}$ cm^2 s^{-1} (measured in this laboratory)] using effective hydrodynamic radii r_i evaluated from the relation[7] $D_i^\infty = kT/4\pi\eta r_i$ recommended for solutions of molecules of similar size. The term k is the Boltzmann constant, and η is the viscosity of pure *n*-dodecane (0.007454 g cm^{-1} s^{-1} at 25 °C).[23]

The D_{12} values predicted by the thermodynamic model (eq 28) are slightly too large. Nevertheless, close agreement with experiment is obtained, generally within (0.01 to 0.02) × 10^{-5} cm^2 s^{-1}. The D_{12} values suggested by the excluded-volume

TABLE 2: Measured Ternary Mutual Diffusion Coefficients[a] for Solutions of *n*-Octane(1) + *n*-Hexadecane(2) in *n*-Dodecane(0) at 25 °C

$\bar{c}_1$	$\bar{c}_2$	D_{11}	D_{12}	D_{21}	D_{22}
0.0874	0.0875	1.181 (0.022)	0.000 (0.014)	0.003 (0.021)	0.679 (0.014)
0.4375	0.4375	1.163 (0.033)	0.028 (0.005)	−0.013 (0.004)	0.690 (0.003)
0.7288	0.7289	1.129 (0.013)	0.048 (0.008)	−0.015 (0.012)	0.708 (0.009)
1.4583	1.4578	1.091 (0.022)	0.083 (0.009)	−0.046 (0.025)	0.737 (0.008)
0.9008	0.4505	1.180 (0.009)	0.061 (0.006)	−0.016 (0.013)	0.743 (0.006)
1.3918	0.4638	1.232 (0.015)	0.094 (0.003)	−0.010 (0.024)	0.791 (0.004)
1.9137	0.4783	1.284 (0.023)	0.130 (0.007)	−0.010 (0.019)	0.848 (0.008)
0.1554	1.8642	0.899 (0.010)	0.008 (0.003)	−0.053 (0.004)	0.587 (0.004)
2.4004	0.2016	1.375 (0.004)	0.172 (0.005)	−0.014 (0.010)	0.934 (0.010)

[a] Estimated standard deviations in parentheses; units: $\bar{c}_i$ in mol dm^{-3}, D_{ik} in 10^{-5} cm^2 s^{-1}.

TABLE 3: Measured and Predicted Values[a] of Cross-Diffusion Coefficient D_{12} for Ternary Solutions of *n*-Octane(1) + *n*-Hexadecane(2) in *n*-Dodecane(0) at 25 °C

$\bar{c}_1$	$\bar{c}_2$	D_{12} (measured)	D_{12} (ideal therm.) eq 28	D_{12} (nonideal therm.) eq 27	D_{12} (excluded vol.) eq 16
0.0874	0.0875	0.000 (0.014)	0.007	0.006	0.084
0.4375	0.4375	0.028 (0.005)	0.034	0.030	0.762
0.7288	0.7289	0.048 (0.008)	0.057	0.049	2.522
1.4583	1.4578	0.083 (0.009)	0.116	0.111	(842.)[b]
0.9008	0.4505	0.061 (0.006)	0.072	0.063	1.636
1.3918	0.4638	0.094 (0.003)	0.116	0.104	2.715
1.9137	0.4783	0.130 (0.007)	0.166	0.151	4.013
0.1554	1.8642	0.008 (0.003)	0.010	0.008	0.937
2.4004	0.2016	0.172 (0.005)	0.219	0.203	3.198

[a] Estimated standard deviations in parentheses; units: $\bar{c}_i$ in mol dm^{-3}, D_{ik} in 10^{-5} cm^2 s^{-1}. [b] The effective volume fraction of *n*-hexadecane exceeds unity at this composition.

TABLE 4: Measured and Predicted Values[a] of Cross-Diffusion Coefficient D_{21} for Ternary Solutions of *n*-Octane(1) + *n*-Hexadecane(2) in *n*-Dodecane(0) at 25 °C

$\bar{c}_1$	$\bar{c}_2$	D_{21} (measured)	D_{21} (ideal therm.) eq 26	D_{21} (nonideal therm.) eq 20	D_{21} (excluded vol.) eq 15
0.0874	0.0875	0.003 (0.021)	−0.004	−0.004	0.002
0.4375	0.4375	−0.013 (0.004)	−0.019	−0.022	0.013
0.7288	0.7289	−0.015 (0.012)	−0.032	−0.036	0.023
1.4583	1.4578	−0.046 (0.025)	−0.064	−0.072	0.052
0.9008	0.4505	−0.016 (0.013)	−0.020	−0.023	0.015
1.3918	0.4638	−0.010 (0.024)	−0.022	−0.025	0.018
1.9137	0.4783	−0.010 (0.019)	−0.023	−0.027	0.020
0.1554	1.8642	−0.053 (0.004)	−0.070	−0.076	0.047
2.4004	0.2016	−0.014 (0.010)	−0.010	−0.012	0.010

[a] Estimated standard deviations in parentheses; units: $\bar{c}_i$ in mol dm^{-3}, D_{ik} in 10^{-5} cm^2 s^{-1}.

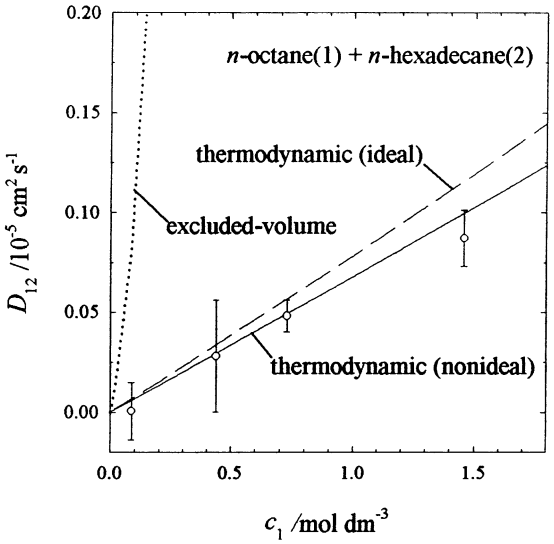

Figure 2. Cross-coefficient D_{12} for equimolar solutions of *n*-octane(1) + *n*-hexadecane(2) (compositions A, B, C, D): ○, measured values; ···, excluded-volume predictions (eq 16); thermodynamic predictions for ideal (− − −, eq 28) and nonideal (—, eq 27) solutions.

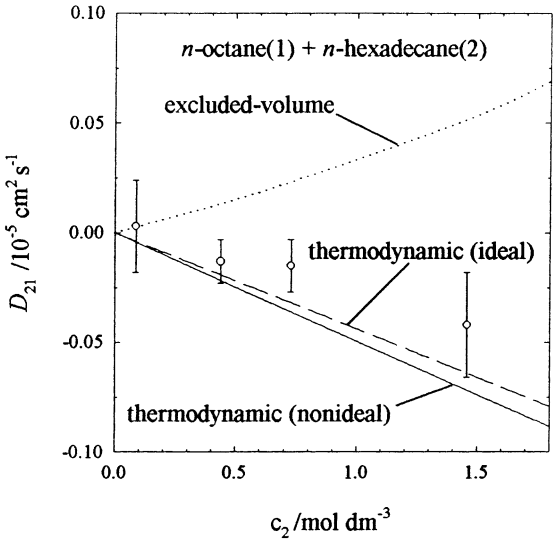

Figure 3. Cross-coefficient D_{21} for equimolar *n*-octane(1) + *n*-hexadecane(2) solutions (compositions A, B, C, D): ○, measured values; ···, excluded-volume predictions (eq 15); thermodynamic predictions for ideal (− − −, eq 16) and nonideal (—, eq 20) solutions.

model (eq 16) are too large and are not in qualitative agreement with experiment. Figure 2 provides a graphical comparison of the measured and predicted D_{12} values for the equimolar *n*-octane(1) and *n*-hexadecane(2) solutions (compositions A, B, C, D).

Table 4 gives the measured and predicted D_{21} values. Good agreement with experiment is obtained for the thermodynamic predictions (eq 26). The excluded-volume D_{21} values (eq 15), however, are several times too large and in this case have the wrong sign. These features are illustrated in Figure 3 for the equimolar *n*-octane(1) + *n*-hexadecane(2) solutions.

Ideal solutions have been assumed up to this point in the analysis. Specifically, the molar volumes of the pure liquids have been used for the partial molar volumes of the solution components. In addition, unit activity coefficients have been assumed, even though several of the solutions are relatively concentrated (>1 mol dm^{-3}). To check the validity of the ideal-solution approximation, the equations developed in the Appendix were used to calculate accurate partial molar volumes[31] and activity coefficients[32] for the *n*-octane(1) + *n*-hexadecane(2) + *n*-dodecane(0) solutions. Tables 3 and 4 give the values of D_{12} and D_{21} predicted by the thermodynamic model for nonideal

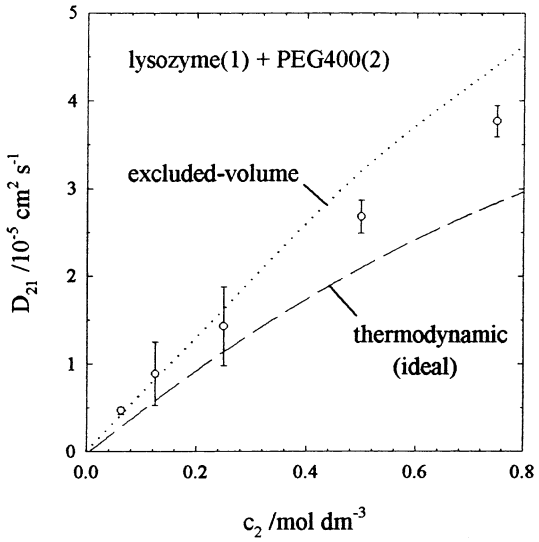

Figure 4. Cross-coefficient D_{21} for aqueous lysozyme(1) + PEG400-(2) solutions: ○, measured values; ···, excluded-volume predictions (eq 15); − − −, thermodynamic predictions assuming ideal solutions (eq 16).

n-octane(1) + *n*-hexadecane(2) + *n*-dodecane(0) solutions (eq 20). As illustrated in Tables 3 and 4 and in Figures 2 and 3, removing the ideal-solution approximation produces relatively small changes in the predicted cross-coefficients ($<0.02 \times 10^{-5}$ cm^2 s^{-1}). Details of the cross-coefficient predictions for nonideal solutions using eq 20 are given in the Appendix.

Aqueous Solutions of Lysozyme(1) + PEG400(2). Vergara et al.[1] have reported ternary mutual diffusion coefficients for aqueous solutions containing 0.600 mmol dm^{-3} lysozyme and 0.0625 to 0.750 mol dm^{-3} PEG400. The large coupled flows of PEG400 were discussed in terms of the excluded-volume effect. The present work suggests, however, that thermodynamics can provide an alternate interpretation of this result.

In Figure 4 the measured and predicted D_{21} values for the lysozyme(1) + PEG400(2) solutions are plotted against the PEG400 concentration. The excluded-volume predictions were made using eq 15 and lysozyme effective molar volumes $V_{1,\text{eff}}$ estimated from binary diffusion coefficients measured for aqueous lysozyme using the relation[8]

$$D(c_1) = D_1^{\infty}(1 - 0.90c_1V_{1,\text{eff}}) \qquad (34)$$

for diffusion in solutions of hard spheres. The D_{21} values predicted by the excluded-volume model are in good agreement (generally within 10%) with experiment. This agreement can be improved or made worse by choosing other definitions[8] of the lysozyme effective volume.

Activity coefficients are not available for aqueous lysozyme + PEG solutions. Consequently, the D_{21} values predicted by the thermodynamic model were calculated assuming ideal solutions (eq 26). The values 10 500 cm^3 mol^{-1} and 340 cm^3 mol^{-1} were used for the lysozyme and PEG400 partial molar volumes, respectively.[1] As shown in Figure 4, the thermodynamic D_{21} values are about 30% lower than the measured values. Several factors might contribute to this discrepancy. Because lysozyme is an electrolyte component, nonideal solution behavior is likely to be more significant than for the *n*-alkane solutions. For the *n*-alkane solutions, including activity coefficients changed the predicted D_{12} and D_{21} values by about 10%. Nonideal solution behavior can also be important for aqueous PEG solutions.[1] These factors are not included in the D_{21} predictions, so the qualitative agreement with experiment shown in Figure 4 can be considered reasonably good. Similar agreement between the excluded-volume and thermodynamic predictions is obtained for D_{21} for aqueous lysozyme(1) + NaCl(2) solutions.[2−4]

TABLE A1: Parameters for the Evaluation of Excess Molar Volumes and Excess Gibbs Functions

		excess volumes		excess Gibbs functions	
i	*k*	a_{ik}/cm^3 mol^{-1}	b_{ik}	a_{ik}/cm^3 mol^{-1} b_{ik}	b_{ik}
1	0	−0.308	−0.282	−0.011	0
0	2	−0.097	−0.094	−0.018	0
1	2	−0.562	−0.752	−0.071	0

Conclusions

Thermodynamics can be used to understand the coupled diffusion of solution components caused by differences in the molecular size. Gradients in the concentration of macromolecular solutes are predicted to drive large co-current coupled flows of other solutes, in good agreement with previously developed excluded-volume theory. For an unambiguous test of the excluded-volume and thermodynamic models of coupled diffusion, ternary mutual diffusion coefficients have been measured for nearly-ideal solutions of *n*-octane(1) + *n*-hexadecane(2) in *n*-dodecane(0). For this system the excluded-volume model fails qualitatively, whereas the cross-diffusion coefficients predicted by the thermodynamic model are in close agreement with experiment. In particular, the thermodynamic model accounts for the counter-current coupled flows of *n*-hexadecane driven by *n*-octane concentration gradients in terms of the smaller volume of *n*-octane molecules relative to the *n*-dodecane solvent.

The thermodynamic treatment of coupled diffusion is consistent with the ORR and it provides a physical explanation for coupled solute diffusion in terms of chemical potential gradient driving forces, without resorting to the concepts of effective concentrations and effective molar volumes. Though limited in scope to ideal or nearly-ideal nonelectrolyte solutions, the thermodynamic model of coupled diffusion developed in this paper can be extended to more complicated systems by including terms for hydration,[12,26,34] association,[35] activity coefficients,[12] ionic migration in diffusion-induced electric fields[12,34,36] and polydispersity.[37]

Acknowledgment. Acknowledgment is made to the Natural Sciences and Engineering Research Council for the financial support of this work.

Appendix

Predicted D_{12} and D_{21} Values for Nonideal Solutions. The relatively small[19,22,23] excess molar volumes[29] ${}^{E}V_{10}$, ${}^{E}V_{02}$, ${}^{E}V_{12}$ and excess molar Gibbs functions[32] ${}^{E}G_{10}$, ${}^{E}G_{02}$, ${}^{E}G_{12}$ for nearly-ideal *n*-octane(1) + *n*-dodecane(0), *n*-dodecane(0) + *n*-hexadecane(2) and *n*-octane(1) + *n*-hexadecane(2) binary mixtures are adequately represented by equations of the form

$${}^{E}Y_{ik} = X_i = X_k\,(a_{ik} + b_{ik}X_i)\;(Y = V \text{ or } G) \qquad \text{(A1)}$$

using the a_{ik} and b_{ik} parameters listed in Table A1. The excess properties of the ternary *n*-octane(1) + *n*-hexadecane(2) + *n*-dodecane(0) mixtures can be evaluated by differentiating the Redlich−Kister equation[33]

$$^{E}Y = X_1X_0\,(a_{10} + b_{10}X_0) + X_0X_2\,(a_{02} + b_{02}X_0) + X_1X_2(a_{12} + b_{12}X_1) \quad \text{(A2)}$$

$$^{E}Y_1 = {}^{E}Y + (1 - X_1)\left(\frac{\partial^E Y}{\partial X_1}\right)_{X_2} - X_2\left(\frac{\partial^E Y}{\partial X_2}\right)_{X_1} \quad \text{(A3)}$$

$$^{E}Y_2 = {}^{E}Y + (1 - X_2)\left(\frac{\partial^E Y}{\partial X_2}\right)_{X_1} - X_1\left(\frac{\partial^E Y}{\partial X_1}\right)_{X_2} \quad \text{(A4)}$$

$$^{E}Y_3 = {}^{E}Y - X_1\left(\frac{\partial^E Y}{\partial X_1}\right)_{X_2} - X_2\left(\frac{\partial^E Y}{\partial X_2}\right)_{X_1} \quad \text{(A5)}$$

Partial molar volumes and activity coefficients for the ternary mixtures are evaluated using $V_i = V_i^* + {}^{E}V_i$ and $^{E}G_i = RT \ln \gamma_i$, where V_i^* denotes the molar volume of pure liquid i.

Further differentiation of the equations for $^{E}G_i$ gives expressions for $\partial \ln \gamma_i/\partial X_k$. The concentration derivatives $\partial \ln \gamma_i /\partial c_k$ required to evaluate the nonideal thermodynamic contributions to the mutual diffusion of the components were evaluated using $X_i = c_i/(c_0 + c_1 + c_2)$, $V_0\, \mathrm{d}c_0 + V_1\, \mathrm{d}c_1 + V_2\, \mathrm{d}c_2 = 0$ and

$$\left(\frac{\partial \ln \gamma_i}{\partial c_k}\right)_{c_l} = \left(\frac{\partial \ln \gamma_i}{\partial X_1}\right)_{c_i}\left(\frac{\partial X_1}{\partial c_k}\right)_{X_2} + \left(\frac{\partial \ln \gamma_i}{\partial X_2}\right)_{c_l}\left(\frac{\partial X_2}{\partial c_k}\right)_{X_1} \quad \text{(A6)}$$

Finally, the concentration derivatives of the chemical potentials were evaluated using

$$\frac{1}{RT}\left(\frac{\partial \mu_i}{\partial c_k}\right)_{c_{m\neq k}} = \left(\frac{\partial \ln X_i}{\partial c_k}\right)_{c_{m\neq k}} + \left(\frac{\partial \ln \gamma_i}{\partial c_k}\right)_{c_{m\neq k}} \quad \text{(A7)}$$

The values of $(\partial \mu_i/\partial c_k)_{c_{m\neq k}}$ calculated in this manner were substituted into eqs 20 and 27 to estimate cross-coefficients D_{12} and D_{21} for nonideal *n*-octane(1) + *n*-hexadecane(2) + *n*-dodecane(0) solutions.

References and Notes

(1) Vergara, A.; Paduano, L.; Sartorio, R. *Macromolecules* **2002**, *35*, 1389.

(2) Vergara, A.; Paduano, L.; Vitagliano, V.; Sartorio, R. *Mater. Chem. Phys.* **2000**, *66*, 126.

(3) Albright, J. G.; Annunziata, O.; Miller, D. G.; Paduano, L.; Pearlstein, J. *J. Am. Chem. Soc.* **1999**, *121*, 3256.

(4) Annunziata, O.; Paduano, L.; Pearlstein, P. J.; Miller, D. G. *J. Am. Chem. Soc.* **2000**, *122*, 5916.

(5) Vergara, A.; Paduano, L.; Vitagliano, V.; Sartorio, R. *Macromolecules* **2001**, *34*, 991.

(6) Roscigno, P.; Paduano, L.; D'Errico, G.; Vitagliano, V. *Langmuir* **2001**, *17*, 4510.

(7) Vergara, A.; Paduano, L.; Sartorio, R. *J. Phys. Chem. B* **2001**, *105*, 328.

(8) Vergara, A.; Paduano, L.; Vitagliano, V.; Sartorio, R. *J. Phys. Chem. B* **2000**, *104*, 8068.

(9) Vergara, A.; Paduano, L.; Sartorio, R. *Phys. Chem. Chem. Phys.* **2001**, *3*, 4340.

(10) Albright, J. G.; Paduano, L.; Sartorio, R.; Vergara, A.; Vitagliano, V. *J. Chem. Eng. Data* **2001**, *46*, 1283.

(11) Tyrrell, H. J. V.; Harris, K. R. *Diffusion in Liquids*; Butterworths: London, 1984.

(12) Robinson, R. A.; Stokes, R. H. *Electrolyte Solutions*, 2nd ed.; Butterworths: London, 1959.

(13) Guggenheim, E. A. *Thermodynamics*, 3rd ed.; North Holland: Amsterdam, 1957.

(14) Baldwin, W. H.; Raridor, R. J.; Kraus, K. A. *J. Phys. Chem.* **1969**, *73*, 3417.

(15) Grunwald, E.; Baughman, G.; Kohnstam, G. *J. Am. Chem. Soc.* **1960**, *82*, 5801.

(16) Cussler, E. L.; Lightfoot, E. N. *J. Phys. Chem.* **1965**, *69*, 1135.

(17) Vitagliano, V.; Sartorio, R. *J. Phys. Chem.* **1970**, *74*, 2949.

(18) Burchard, J. K.; Toor, H. L. *J. Phys. Chem.* **1962**, *66*, 2015.

(19) Kett, T. K.; Anderson, D. K. *J. Phys. Chem.* **1969**, *73*, 1268.

(20) Havenga, E.; Leaist, D. G. *J. Chem. Soc., Faraday Trans.* **1998**, *94*, 3353.

(21) Miller, D. G. *Chem. Rev.* **1960**, *60*, 15.

(22) Van Geet, A. L.; Adamson, A. W. *J. Phys. Chem.* **1964**, *68*, 238.

(23) Shieh, J. C.; Lyons, P. A. *J. Phys. Chem.* **1969**, *73*, 3258.

(24) Cussler, E. L. *Multicomponent Diffusion*; Elsevier: Amsterdam, 1957.

(25) Cussler, E. L.; Breuer, M. M. *AIChE J.* **1972**, *18*, 812.

(26) Leaist, D. G. *J. Chem. Soc., Faraday Trans.* **1991**, *76*, 597.

(27) Deng, Z.; Leaist, D. G. *Can. J. Chem.* **1991**, *69*, 1584.

(28) Havenga, E.; Leaist, D. G. *J. Chem. Soc., Faraday Trans.* **1998**, *94*, 3353.

(29) Agar, J. N. *Trans. Faraday Soc.* **1960**, *56*, 776.

(30) Dunlop, P. J.; Gosting, L. J. *J. Phys. Chem.* **1959**, *63*, 86.

(31) Aucejo, A.; Cruz Burguet, M.; Muñoz, R.; Marques, J. L. *J. Chem. Eng. Data* **1995**, *40*, 141.

(32) Lo, H. Y. *J. Chem. Eng. Data* **1974**, *19*, 236.

(33) Acree, W. E. *Thermodynamic Properties of Nonelectrolyte Solutions*; Academic: New York, 1984.

(34) Leaist, D. G.; Curtis, N. *J. Solution Chem.* **1999**, *28*, 341.

(35) Leaist, D. G. *Phys. Chem. Chem. Phys.* **2002**, *4*, 4732.

(36) Leaist, D. G.; Hao. L. *J. Chem. Soc., Faraday Trans.* **1993**, *89*, 2775.

(37) MacEwan, K.; Leaist, D. G. *J. Phys. Chem. B* **2001**, *106*, 10296.